

2022

Flow Boiling Heat Transfer Characteristics Of Water For Metal-Foam-Filled Horizontal Tube

Cheng-Min Yang

Kashif Nawaz

Anthony Gehl

Follow this and additional works at: <https://docs.lib.purdue.edu/iracc>

Yang, Cheng-Min; Nawaz, Kashif; and Gehl, Anthony, "Flow Boiling Heat Transfer Characteristics Of Water For Metal-Foam-Filled Horizontal Tube" (2022). *International Refrigeration and Air Conditioning Conference*. Paper 2396.
<https://docs.lib.purdue.edu/iracc/2396>

This document has been made available through Purdue e-Pubs, a service of the Purdue University Libraries. Please contact epubs@purdue.edu for additional information. Complete proceedings may be acquired in print and on CD-ROM directly from the Ray W. Herrick Laboratories at <https://engineering.purdue.edu/Herrick/Events/orderlit.html>

Flow Boiling Heat Transfer Characteristics of Water for Metal-foam-filled Horizontal Tubes

Cheng-Min YANG¹, Kashif NAWAZ^{1*}, Anthony GEHL¹

¹ Oak Ridge National Laboratory, Building Technologies Research and Integration Center (BTRIC),
Oak Ridge, TN, USA
Contact Information (yangc1@ornl.gov; nawazk@ornl.gov)

* Corresponding Author

ABSTRACT

The goal of this paper is to enhance the in-tube flow boiling heat transfer of water while accounting for potential increase in pressure drop. Metal foams are a class of cellular structure with large surface-area-to-volume ratio and tortuous structure which has shown promising results for various energy conversion and storage applications. The higher heat transfer area and higher nucleation sites density due to the porous media can effectively enhance the heat transfer of water in both single-phase and two-phase operations. This paper presents the local heat transfer and pressure drop measurements of water in a partially metal-foam-filled horizontal copper tube. The ranges of parameters in the experiments are: mass flux from 80 to 200 kg/s-m², heat flux from 3.5 to 105 kW/m², and vapor quality from subcooled to 0.3. The results in the metal-foam-filled tube are compared with that of the bare copper tube. The effect of metal foam on the thermal hydraulic characteristics is discussed and analyzed. In addition, the two-phase flow behavior in a transparent tube filled with the same metal foam was visualized and investigated by high-speed imaging system. The experiments were also conducted in the tube without the metal foam for comparison.

1. INTRODUCTION

The development of high-efficient thermal conversion system has been an ongoing effort. Among various transport processes in applications such as power generation, desalination, and HVAC&R, evaporation is often a performance-limiting process. Cost-effective evaporation processes can not only reduce the footprints and capital cost of the equipment but also enable a major reduction in operation and maintenance costs. To enhance the performance of evaporators or boilers, several active and passive techniques have been investigated. Individual approaches can vary in terms of the potential impact, cost of deployment, and scalability. Internal enhancement for improved flow boiling is a proven technology where numerous types of micro fin have been studied for the impact on thermal-hydraulic performance. Due to promising performance, such enhancements have been extensively deployed in a range of flow boiling processes (Mousa et al., 2021). The interaction of working fluids with micro fin has been a subject of interest where a broad range of analytical, experimental, and visualization analyses has been conducted. While such enhancements have shown performance improvement, further improvements are needed due to technological challenges. Particularly, in HVAC&R applications, the development of compact equipment has become a challenge and in many cases is a major hurdle for deployment.

The use of metal foams as high surface area enhancement has been explored for a range of thermal applications such as air to air and air to refrigerant heat transfer (Nawaz, 2012). The unprecedented surface area per unit volume, complex cell structure and availability of high-density nucleation sites have enabled solutions with remarkable thermal-hydraulic performance (Nawaz et al., 2017). Therefore, deploying porous media inside the tube is one potential approach to attain unprecedented performance improvement of flow boiling. The wicking effect due to small cell size also ensures that dry out at the wall can be avoided and assist with pre-initialization of annular flow which leads to a higher heat transfer coefficient. Zhao et. al (2009) experimentally investigated the flow boiling heat transfer

Notice: This manuscript has been authored in part by UT-Battelle, LLC, under contract DE-AC05-00OR22725 with the US Department of Energy (DOE). The US government retains and the publisher, by accepting the article for publication, acknowledges that the US government retains a nonexclusive, paid-up, irrevocable, worldwide license to publish or reproduce the published form of this manuscript, or allow others to do so, for US government purposes. DOE will provide public access to these results of federally sponsored research in accordance with the DOE Public Access Plan (<http://energy.gov/downloads/doe-public-access-plan>).

of R134a in horizontal tubes filled with copper foam. Their results showed that the heat transfer coefficient of the foam tubes was approximately three times higher than that of the plain tube. Zhu et al. (2014) studied the flow boiling heat transfer characteristic of R410A in a tube filled with copper foam. The experimental results revealed that the metal foam was able to promote the flow pattern transition from stratified wavy flow to annular flow and enhance the heat transfer by up to 220%. Regardless, this technique is expected to enhance the heat transfer of flow boiling water and revolutionize the boiler industry by providing a highly compact solution for challenging applications. Most of the related studies in the literature utilized refrigerants as the working fluid.

The objective of the present experimental study is to investigate the flow boiling heat transfer and pressure drop of water in a horizontal metal-foam-filled tube. Instead of deployment as filler materials inside the tube, a highly compressed foam layer is only positioned at the periphery of the tubes. Such deployment ensures that pressure drop through the tube is acceptable while ensuring that appropriate improvement in heat transfer can be observed. In addition, the two-phase flow behavior in a transparent tube filled with the same metal foam was visualized to help understanding the heat transfer mechanisms.

2. DESCRIPTION OF EXPERIMENTS

2.1 Experimental Apparatus

The experimental apparatus used in this study is to measure the in-tube heat transfer coefficient and pressure drop of flowing water for both liquid-phase and boiling conditions. Figure 1 shows a schematic diagram of the experimental setup used in this study. It consists of a water reservoir, a gear pump, a Coriolis mass flow meter, a pre-conditioning section, a developing section, a test section, a visualization section, and a chiller. The distilled water is the working fluid for the current study, and it is preheated and stored in a 2.5-gallon tank-type water heater. The water is pumped to the flow loop through a gear pump, and an additional by-pass loop back to the tank is designed for flow rate control. The mass flow rate of water flowing into the main line is measured with a Coriolis flow meter, and a strainer with 150-mesh screen (89 μm) is installed to catch debris and protect the equipment. There are three main sections in the flow loop: pre-heating section, flow development section and heat transfer test section. The pre-heating section is used to provide the desired conditions (temperature or vapor quality) for the heat transfer test section. The heating power is provided and controlled through six 1.5 kW band heaters. The flow development section is a 1 m long copper tube, which enables the water to reach fully developed flow. It is fully insulated to minimize the heat loss, and thus this section is nearly adiabatic. The heat transfer test section is the measurement section for the heat transfer coefficient and pressure drop for tube samples. The heat flux in the test section is supplied and controlled through two 1.5 kW band heaters. After the test section, there is a clear FEP tubing for visualizing the two-phase flow pattern, which helps understanding the simultaneous motion of liquid and vapor flows. Then, the steam-water mixture is condensed in a plate heat exchanger and directed back to the reservoir.

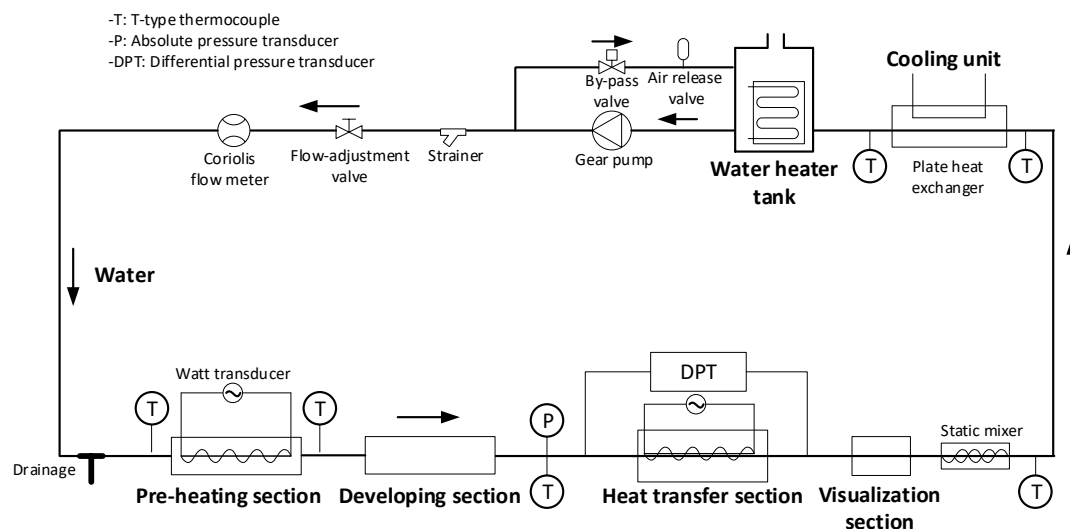


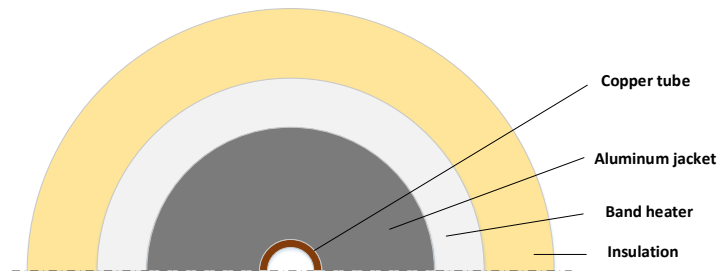
Figure 1: Schematic of test apparatus

In the facility, the fluid temperatures were measured using T-type thermocouples. The wall temperatures in the heat transfer test section were measured with K-type thermocouples. All thermocouples were calibrated with an accuracy of ± 0.1 °C. The mass flow rate of water was measured by a Coriolis mass flow meter with a range of 0.001 to 0.03 kg/s with an accuracy of $\pm 0.20\%$ of the reading. The absolute pressure of water was determined by an absolute pressure transducer with an accuracy of ± 0.31 kPa. Horizontal pressure drop of the tested tubes within the test section were measured by differential pressure transducers with an accuracy of ± 5.52 Pa. The electrical power inputs to the pre-heating section and heat transfer sections were determined using watt transducers with 0.5% reading accuracy. The measured data from thermocouples, mass flow meter, pressure transducers, and watt transducer was collected by a data logger every 1 second.

2.2 Heat Transfer Test Section and Internally Enhanced Tube

The heat transfer test section consists of a test tube, two half-piece aluminum jackets, and two electric band heaters, as illustrated in Figure 2(a). The test tube is a 3/8" OD copper tube with a heated length of 30 cm. The inner diameter and outer diameters are 7.89 and 9.53 mm, respectively. Around the outer surface are two half-piece cylindrical shape aluminum jackets, which are used to provide a more uniform heat flux condition and temperature distribution. All the gaps between the two aluminum pieces and the copper tube are filled with high thermal conductivity paste to reduce the thermal contact resistance. The required heat flux to the working fluid is generated through two electric band heaters. The heating power of each heater is 1.5 kW, and each heater is insulated with a 1/4" thick ceramic fiber insulating blanket. The built-in blanket comes with three screws for clamping the heat transfer assembly. The heat transfer test section is insulated with a 2" thick fiberglass pipe insulation. Additionally, there are four grooves on each aluminum jacket designed for placing thermocouples, and the locations of the wall temperature measurement and the longitudinal view of the aluminum jacket are illustrated in Figure 2(b). The wall temperatures are measured at four locations along the axis of the heated section with an equal interval of 60 mm. For each location, four thermocouples are equally distributed over the circumference and attached at the outer wall of the test tube. In total, sixteen points on the tube surface are measured and used for the heat transfer calculation. More details regarding the design of the aluminum jacket can be referred to the previous work of Yang and Hrnjak (2018). The internally enhanced tube for the current study was made in-house by attaching a thin layer of aluminum foam to the internal surface of a copper tube. The aluminum foam used in the sample is 40 PPI, 4-6% density range, and compressed to 0.05" thickness with 22.62% actual density. The aluminum foam was first rolled to a circular shape and placed inside the copper tube. Then, a round tube with 5/16" was inserted into the tube and press the foam to have a better contact with the internal surface. Figure 3 demonstrates the metal-foam-filled tube, and it is seen that the aluminum foam successfully contacts the tube surface.

(a)



(b)

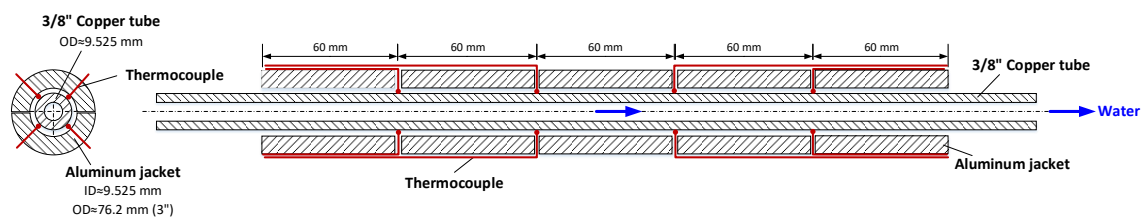


Figure 2: (a) Cross sectional view of the heat transfer test section and (b) locations of thermocouples

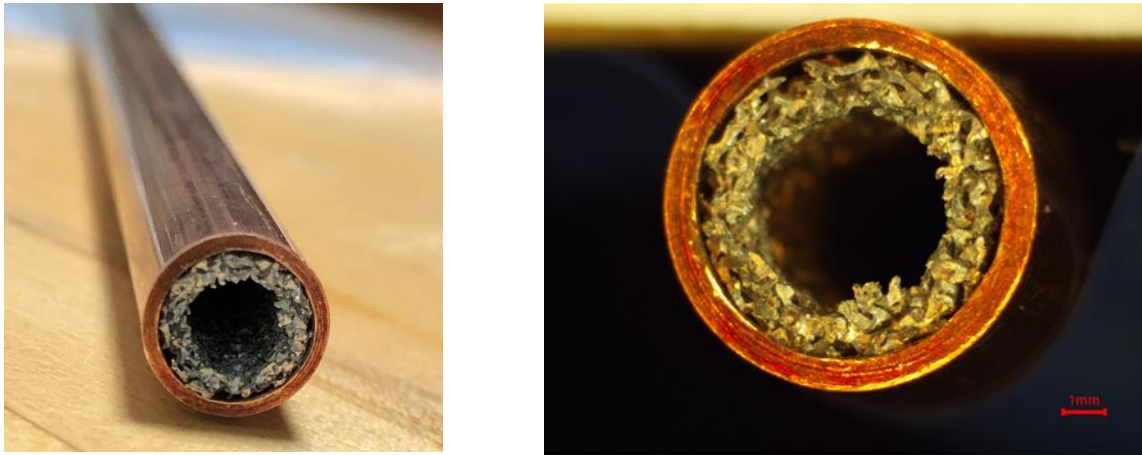


Figure 3: Metal-foam-filled internally enhanced tubes

3. DATA REDUCTION

3.1 Pressure Drop

The two-phase frictional pressure drop through the tested tube during evaporation is determined from a combination of the measured differential pressure (total pressure drop), acceleration pressure drop, static pressure drop, and the calculated minor losses.

$$\Delta P_{tot} = \Delta P_{fric} + \Delta P_{acc} + \Delta P_{static} + \Delta P_{loss} \quad (1)$$

The acceleration pressure gain is estimated through the change in kinetic energy of flow using the separated flow model, as described in Eq. (2).

$$\Delta P_{acc} = G^2 \left\{ \left(\frac{(1-x)^2}{\rho_l(1-\alpha)} + \frac{x^2}{\rho_v\alpha} \right)_o - \left(\frac{(1-x)^2}{\rho_l(1-\alpha)} + \frac{x^2}{\rho_v\alpha} \right)_i \right\} \quad (2)$$

where x is vapor quality, α is void fraction, ρ_v is vapor density, ρ_l is liquid density, and G is mass flux.

The inlet and outlet void fractions are calculated through the Steiner (1993) version of Rouhani and Axelsson model.

$$\alpha = \frac{x}{\rho_v} \left[\left(1 + 0.12(1-x) \right) \left(\frac{x}{\rho_v} + \frac{(1-x)}{\rho_l} \right) + \frac{1.18(1-x) \left[g\sigma(\rho_l - \rho_v) \right]^{0.25}}{G\rho_l^{0.5}} \right]^{-1} \quad (3)$$

The static pressure drop is expressed as

$$\Delta P_{static} = (\rho_v\alpha + \rho_l(1-\alpha))gl \sin(\theta) \quad (4)$$

where g is the gravitational acceleration, l is the length of the test tube, and θ is the inclination angle of the channel. For a horizontal tube, the change of static head is 0.

The minor loss due to the connections of the test tube and the fittings at the entrance and exit is estimated through the following equation.

$$\Delta P_{loss} = K_{loss} \left(\frac{\rho_j V_j^2}{2} \right) \quad (5)$$

where the subscript j represents the phase of the fluid, and V and ρ are the bulk velocity and density of the fluid, respectively. K_{loss} is the loss coefficient, and it is taken from Idelchik (1994).

As a result, the two-phase frictional pressure drop can be obtained by subtracting the acceleration term and minor loss from the measured total pressure drop (Eq. (1)), which is then used for comparison with some classical correlations.

3.2 Heat Transfer Coefficient

The heat transfer coefficient HTC of the water in the test tube is obtained as the ratio of the heat flux to the temperature difference between the wall and water.

$$HTC = \frac{\dot{Q}_{ts}}{A_s (T_{wall} - T_{sat})} \quad (6)$$

where \dot{Q}_{ts} is the heat flow rate transferred to the water and calculated based on the energy balance in the heat transfer test section.

$$\dot{Q}_{ts} = \dot{Q}_{elc,ts} - \dot{Q}_{amb,ts} - \dot{Q}_{cond} \quad (7)$$

where $\dot{Q}_{elc,ts}$ is the heating power of the band heaters in the heat transfer test section, and $\dot{Q}_{amb,ts}$ is the heat loss into the environment from the test section estimated through a calibration experiment. The single-phase test with a wide range of inlet water temperatures were conducted to determine the dependence of heat loss on the temperature difference between the water to the surrounding. During the heat loss test, the band heaters in the test section were turned off. The mass flow rate and the temperature change of liquid water within the test section were measured. The overall heat loss coefficient was calculated by the heat transfer rate and the log mean temperature difference between the water and the ambient air. \dot{Q}_{cond} is the axially conductive heat loss through the copper tube wall, which is attributed to the higher wall temperature in the test section than that away from the test section. It is estimated by a finite element method proposed by Jang and Hrnjak (2004).

The surface area of the test tube, A_s , is calculated using the inner diameter and the heated length. The average inner wall temperature, T_{wall} , is obtained from the average values of the sixteen thermocouples on the outer wall of the test tube and corrected to the corresponding wall temperature at the inner wall surface through 1-D heat conduction equation. The local saturation temperature, T_{sat} , is determined based on the measurement of saturation pressure P_{sat} . The local pressure in the middle of the heat transfer test section is obtained by assuming a linear profile of the pressure between the inlet and outlet. For the current test facility, the pressure transducer is installed at the inlet of the heat transfer section, and thus the local saturation temperature is estimated through Eq. (8).

$$T_{sat} = f(P_{sat,in} - (\Delta P_{tot}/2)) \quad (8)$$

3.3 Operating Conditions

During the single-phase and two-phase experiments, the parameters of the operating condition are heat flux, mass flux and vapor quality, which will be defined in this subsection. In the heat transfer test section, heat flux is the heat transfer rate to the fluid per unit area, and it is calculated as the following equation.

$$q_{ts} = \frac{\dot{Q}_{ts}}{\pi D_i L} \quad (7)$$

where D_i is the inner diameter, and L is the heated length of the test tube.

The mass flux of the water in the test tube G is calculated as

$$G = \frac{\dot{m}_w}{A_c} \quad (8)$$

where \dot{m}_w is the mass flow rate of water, and A_c is the cross-sectional area of the test tube.

$$A_c = \frac{\pi D_i^2}{4} \quad (9)$$

The inlet vapor quality of the steam-water mixture at the inlet of the test section is controlled by the band heaters in the pre-heating section. The subcooled water enters the preheating section and is heated until the desired vapor quality is reached. The thermodynamic vapor quality at the inlet of test section can be estimated through the energy balance

$$x_{ts,i} = \frac{\dot{Q}_{pre} - \dot{m}_w C_{p,w} (T_{pre,o} - T_{pre,i})}{\dot{m}_w h_{fg}} \quad (10)$$

where \dot{Q}_{pre} is the heat transfer to the water in the preheating section, \dot{m}_w is the mass flow rate of the water, $C_{p,w}$ is the specific heat of the water at the constant pressure, $T_{pre,i}$ and $T_{pre,o}$ are the temperature at the inlet and outlet of the preheating section, and h_{fg} is the latent heat of the water.

$$\dot{Q}_{pre} = \dot{Q}_{elc,pre} - \dot{Q}_{amb,pre} \quad (11)$$

where $\dot{Q}_{elc,pre}$ is the heating power of the band heaters in the preheating section and $\dot{Q}_{amb,pre}$ is the heat loss into the environment from the preheating section. The heat leak from the preheating section through the insulators were measured through the single-phase calibration experiments. Similarly, the vapor quality of the steam-water mixture at the outlet of the test section is determined with following equation.

$$x_{ts,o} = x_{ts,i} + \frac{\dot{Q}_{w,ts}}{\dot{m}_w h_{fg}} \quad (12)$$

The mean vapor quality of the water in the heat transfer test section, x_{ts} , is calculated using the arithmetic mean value of outlet and inlet qualities given in Eq. (10) and (12).

$$x_{ts} = \frac{x_{ts,i} + x_{ts,o}}{2} \quad (13)$$

4. RESULTS AND DISCUSSION

4.1 Single-Phase Validation

Prior to the flow boiling tests, the single-phase liquid experiments were performed in a smooth copper tube to validate the test facility. During the validation experiments, the water temperature at the inlet of the test section was controlled at 57°C, and the mass flux varied from 100 to 600 kg/s-m². The measured heat transfer coefficient for the smooth tube at the heat fluxes of 9.64 kW/m², 25.8 kW/m², and 38.5 kW/m² are shown in Figure 4 (a). With increasing mass flux, the heat transfer coefficient increases. As expected, the heat flux does not have a remarkable influence on the heat transfer coefficient. The predicted values from the correlations developed by Dittus and Boelter (1930) and Gnielinski (1976) are also included in Figure 4(a) for further comparison. The experimental data in the turbulent region are generally in line with Gnielinski's correlation. The correlation of Dittus and Boelter overpredicts the heat transfer coefficient because it was originally developed and validated for the Re > 10000. However, the maximum Re is around 6000 in the current experiments. The pressure drop in a horizontal smooth copper tube was measured in separate experiments under adiabatic conditions. The results show in good agreement with the calculated values from Hagen-Poiseuille flow and Blasius equation, as presented in Figure 4 (b). This provides confidence in the validity and reliability of the current test facility.

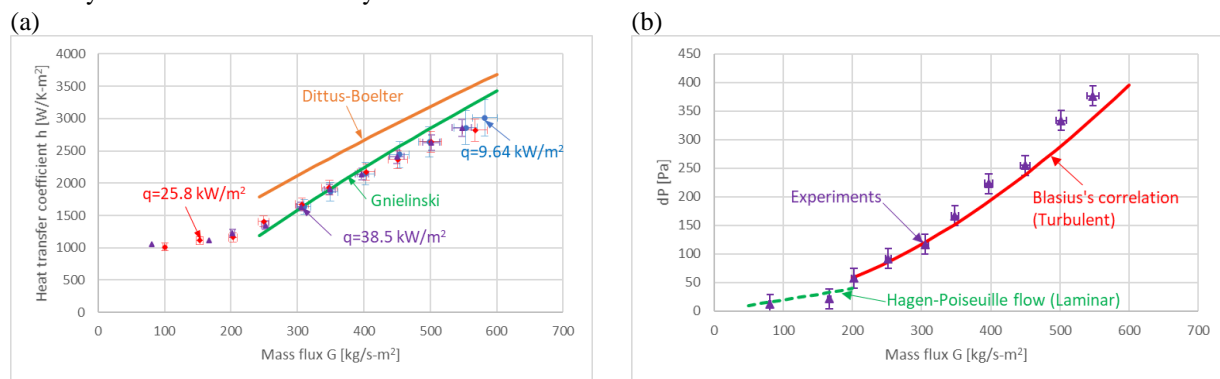


Figure 4: Comparison of the (a) heat transfer coefficient and (b) pressure drop of the liquid water inside smooth tubes with the correlations at different mass fluxes

4.2 HTC and Pressure Drop of Liquid Water in Internally Enhanced Tubes

The convective heat transfer of liquid water in the internally enhanced tube is also important for water heating applications. Figure 5 (a) and (b) present the comparisons of heat transfer coefficient and pressure drop in smooth and metal-foam-filled tubes under single-phase conditions. The inlet temperature of the heat is set at 54°C, and the heat flux is 34 kW/m². Metal foam enhances the liquid-phase heat transfer by 20% to 80%, which depends on mass flux

condition. A higher surface area and enhanced flow mixing leads to a better thermal performance. The heat transfer enhancement ratio is quite constant as the mass flux is higher than 180 kg/s-m^2 . Nevertheless, the pressure drop penalty due to the metal foam is significantly high, especially at high mass velocity. The pressure drop penalty ranges from 3.67 to 23.7, but it seems there exists an optimal operating condition for this prototype tube.

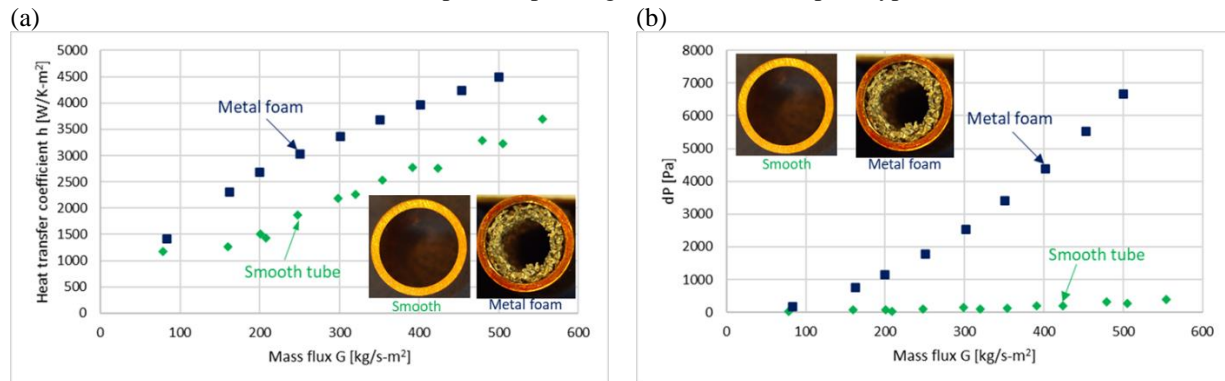


Figure 5: Comparison of (a) heat transfer coefficient and (b) pressure drop of liquid water at various mass fluxes between the metal-foam-filled and smooth tubes

4.3 HTC and Pressure Drop of Flow Boiling Water in Internally Enhanced Tubes

Figure 6 (a) and (b) show the effect of mass flux on pressure drop and heat transfer coefficient in the metal-foam-filled tube, respectively. In the series of experiments, the heat flux is set at 34 kW/m^2 with various vapor qualities. As expected, higher friction at the case of $G=200 \text{ kg/s-m}^2$ leads to a larger pressure drop within the test section, as shown in Figure 6(a). In addition, the pressure drop increases with the increase of vapor quality due to a higher vapor velocity. Figure 6(b) shows the variation in the heat transfer coefficient with vapor quality at three mass fluxes. It is seen that the heat transfer coefficient keeps a steady rising as the vapor quality increases. It also increases with the rise of mass flux due to stronger convective effect. Figure 7 (a) and (b) present the influences of heat flux on pressure drop and heat transfer coefficient, respectively. The experiments were conducted at $G=80 \text{ kg/s-m}^2$ and $x=0.134$ with the heat fluxes from 3.39 to 104 kW/m^2 . The pressure drop increases with increasing heat flux, and this is attributed to a higher vaporization and the acceleration of the fluid more within the test section. The heat transfer coefficient generally increases as the heat flux increases. The heat flux has a stronger impact on heat transfer coefficient as it is lower than 20 kW/m^2 .

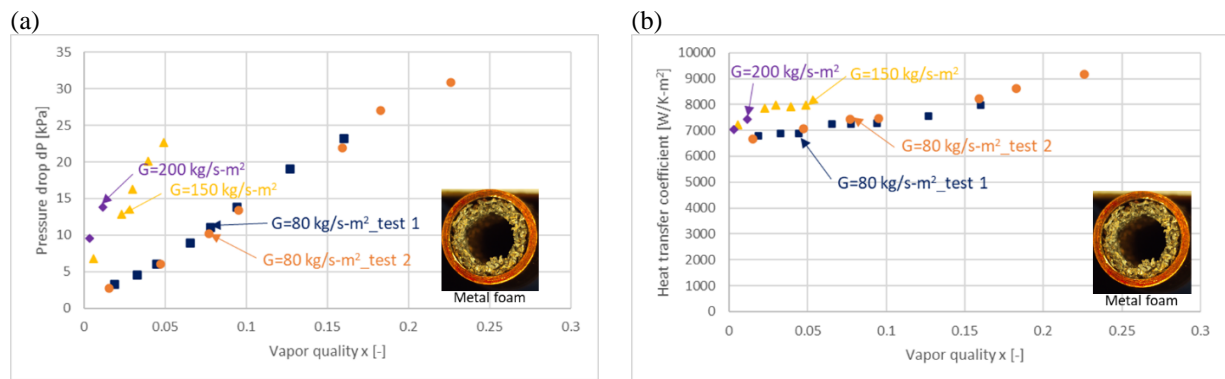


Figure 6: Water flow boiling in the metal foam tube at various mass fluxes: (a) pressure drop and (b) heat transfer coefficient.

For better understanding the overall effect of the metal foam on the in-tube flow boiling of water, the heat transfer and pressure drop of two data sets are compared with the plain tube and presented in Figure 8. The experiments were performed at $G=80 \text{ kg/s-m}^2$, $q=34 \text{ kW/m}^2$, and $x=0$ to 0.25 . Compared to the two data sets measured in the metal-foam-filled tube (blue symbols and orange symbols), the repeatability for both heat transfer and pressure drop data are good. Figure 8(a) shows the comparison of the heat transfer coefficient in two tubes at various vapor qualities. There is no remarkable effect of metal foam on heat transfer as the vapor quality is lower than 0.1 , where the flow

pattern is intermittent (plug or slug). In the annular flow regime, the metal foam effectively enhances the heat transfer rate. The heat transfer enhancement of the metal-foam-filled tube ranges from 1.03 to 1.36 under the current test conditions. The pressure drop penalty factor, however, is considerably high, which is between 19.3 to 26.7, as shown in Figure 8(b). To be noted that the heat transfer enhancement factor of the prototype tube is expected to increase if a better joining method is deployed. Reducing the thermal contact resistance between the foam and inner surface of the tube can maximize the heat transfer capacity. The pressure drop penalty can also be reduced by redesigning and optimizing the metal foam geometry (such as foam thickness and porosity) for the current application.

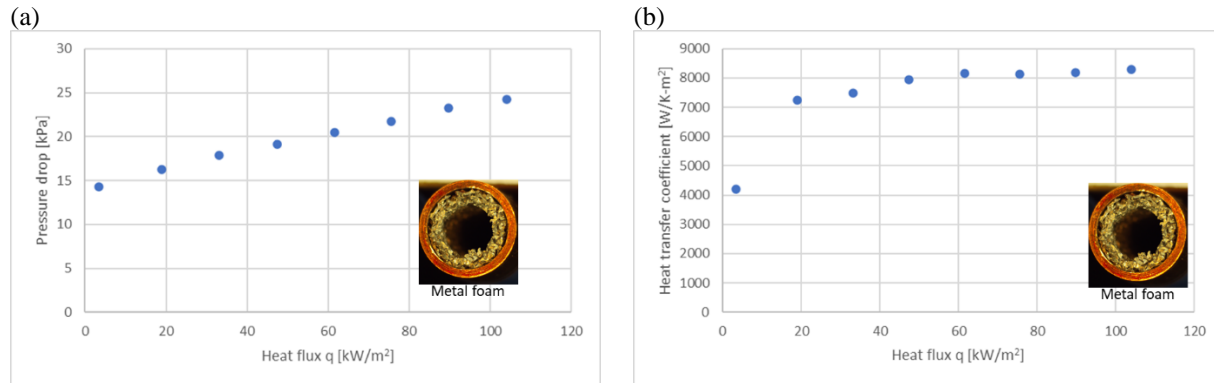


Figure 7: Effect of heat flux on (a) heat transfer coefficient and (b) pressure drop of water in the metal-foam-filled tube ($G=80 \text{ kg/s-m}^2$, $x=0.134$).

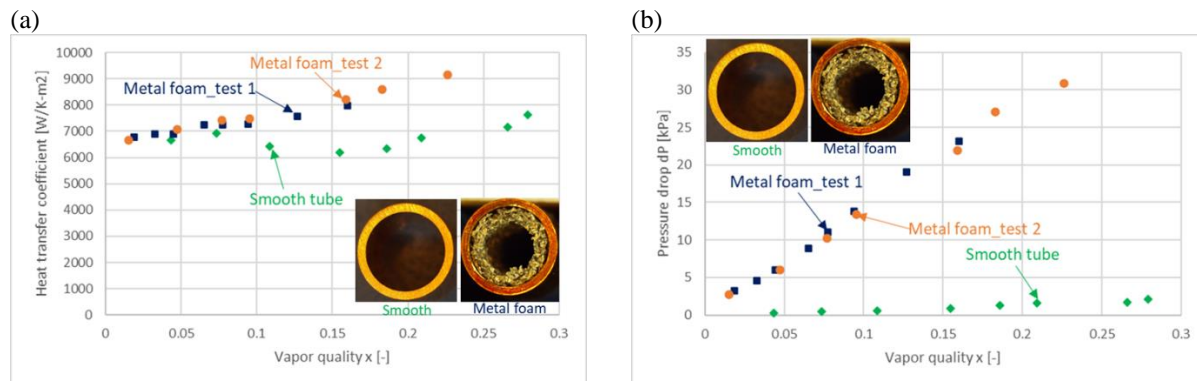


Figure 8: Comparison of (a) heat transfer coefficient and (b) pressure drop of smooth and metal foam tubes under flow boiling conditions at various vapor qualities ($G=80 \text{ kg/m}^2$, $q=34 \text{ kW/m}^2$).

4.4 Visualization of Two-phase flow

The two-phase flow patterns of water for the metal foam enhanced tube were visualized with two different methods. The first method is the traditional sight-glass method, which is a clear empty tube installed at the downstream of the tested metal foam tube for recognizing the flow regime. To further simulate the flow behavior inside the enhanced tube, a thin layer of aluminum foam structure was attached to the internal surface of a transparent FEP tube and the two-phase flow was visualized under the same operating conditions. Plug flow, slug flow, wavy annular flow, and annular flow were observed in the current test conditions, as demonstrated in Figure 9. The definition of each flow pattern can be found in the previous study done by Yang and Hrnjak (2019). The flow direction for each image is from left to right. The metal foam structure in this study does not change the transitions of main flow patterns compared to the smooth tube, but it influences the local flow behavior near the foam structure. Some differences between the empty tube and metal-foam-filled tube were observed. For the plug or slug flow in the metal-foam-filled tube, the big vapor pocket is broken into several small bubbles when the two-phase flow travels through the foam structure. Regarding the annular flow in the metal-foam-filled tube, a continuous liquid film along the periphery of the inner tube surface is disturbed by the foam structure and decelerate. Some bubbles trapped in the pore of the metal foam are occasionally seen.

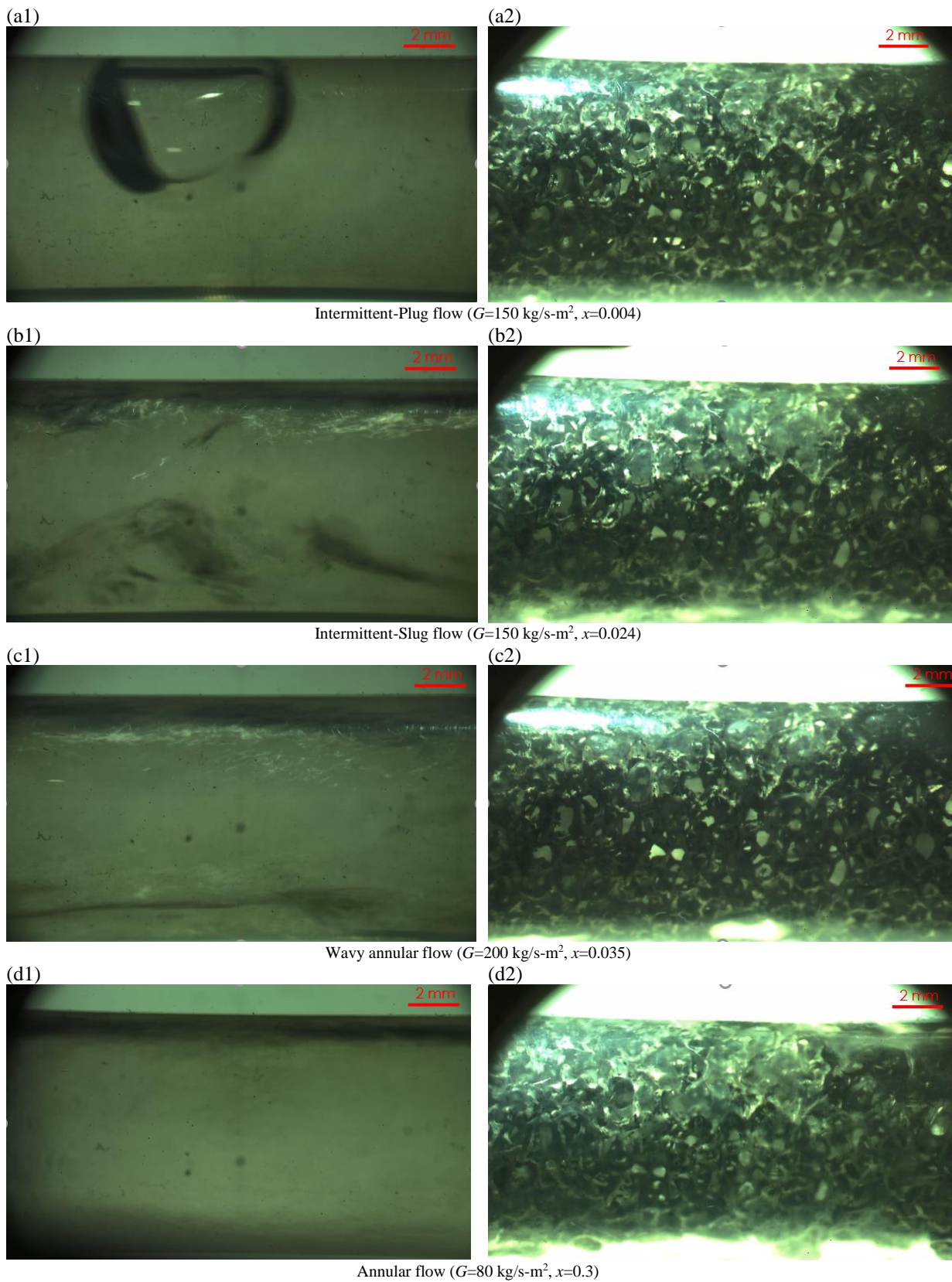


Figure 9: Visualized two-phase flow patterns at the downstream of the metal foam enhanced tube: (a) Plug flow (b) Slug flow, (c) Wavy annular, and (d) Annular flow

5. SUMMARY

This study experimentally investigated the heat transfer coefficient and pressure drop of water inside a metal-foam-filled horizontal tube under liquid-phase and flow boiling conditions. Parametric studies were performed with various heat fluxes, mass fluxes, and vapor qualities, and the results were compared with that of the bare copper tube. Besides, the two-phase flow behavior in the metal-foam-filled tube was also visualized. The key results are summarized below:

- Metal foam effectively enhances the liquid-phase heat transfer by 20% to 80% in the current study, and the enhancement depends on mass velocity. A higher surface area and enhanced flow mixing leads to a better thermal performance. Nevertheless, the pressure drop penalty due to the metal foam is significantly high.
- For the flow boiling of water, the heat transfer enhancement of the metal-foam-filled tube ranges from 1.03 to 1.36 under the current test conditions. For the intermittent flow regime, there is no remarkable difference on the heat transfer between the smooth and enhanced tubes. When the annular flow dominates, the metal foam effectively enhances the heat transfer rate.
- Various flow patterns including slug flow, plug flow, wavy-annular flow, and annular flow were observed in the metal-foam-filled tube. The metal foam structure in this study does not change the transitions of main flow patterns, but it influences the local flow behavior near the foam structure.

REFERENCES

- Dittus, F., & Boelter, L. (1930). Heat transfer in automobile radiators of the tubular type. University of California Publications in Engineering, 2, 443–461.
- Gnielinski, V. (1976). New equations for heat and mass transfer in turbulent pipe and channel flow. *Int. Chem. Eng.*, 16(2), 359–368.
- Idelchik, I. E. (1994). *Handbook of Hydraulic Resistance*, 3rd. ed., Chapters 3 and 4 CRC Press.
- Jang, J., & Hrnjak, P. (2004). Condensation of CO₂ at low temperatures. ACRC Report CR-56.
- Mousa, M. H., Yang, C. M., Nawaz, K., & Miljkovic, N. (2021). Review of heat transfer enhancement techniques in two-phase flows for highly efficient and sustainable cooling. *Renewable and Sustainable Energy Reviews*, 111896.
- Nawaz, K. (2012). Metal foams as novel materials for air-cooling heat exchangers.
- Nawaz, K., Bock, J., & Jacobi, A. M. (2017). Thermal-hydraulic performance of metal foam heat exchangers under dry operating conditions. *Applied Thermal Engineering*, 119, 222-232.
- Steiner, D. (1993). Heat transfer to boiling saturated liquids in: *VDI Heat Atlas*.
- Yang, C. M., & Hrnjak, P. (2018). Effect of straight micro fins on heat transfer and pressure drop of R410A during evaporation in round tubes. *International Journal of Heat and Mass Transfer*, 117, 924-939.
- Yang, C. M., & Hrnjak, P. (2019). Visualization of two-phase flow of R410A in horizontal smooth and axial micro-finned tubes. *International Journal of Heat and Mass Transfer*, 138, 49-58.
- Zhao, C. Y., Lu, W., & Tassou, S. A. (2009). Flow boiling heat transfer in horizontal metal-foam tubes. *Journal of heat transfer*, 131(12).
- Zhu, Y., Hu, H., Sun, S., & Ding, G. (2014). Heat transfer measurements and correlation of refrigerant flow boiling in tube filled with copper foam. *International journal of refrigeration*, 38, 215-226.

ACKNOWLEDGEMENT

The authors are grateful to the colleagues at Oak Ridge National Laboratory who provided useful comments and suggestions to improve the quality of the paper. The authors also acknowledge the support provided by US Department of Energy Building Technologies Office and the technology manager, Mr. Antonio Bouza.